tribution of this study is to confirm the presence of two motions while limiting the type of reorientations which may be proposed.

In attempting to understand a property like impact resistance, the prospect of two overlapping low-temperature motions is important. It might be difficult to account for impact resistance solely on the basis of local, isolated phenylene group rotation over a relatively low intramolecular barrier,[21] but an associated intermolecular process with a potentially longer range character provides a more plausible ingredient. The second, long-range motion may depend on the presence of rapid phenylene group rotation or oscillation, thus linking impact resistance to phenylene group motion as has been proposed.

Questions as yet unanswered are the precise extent of phenylene group rotation or oscillation and the exact nature of the second process. The amount of narrowing of the ^{1}H NMR line tends to indicate fairly large amplitude oscillation if not rotation but another approach will be required to quantify this statement. This is because the dominant dipolar interaction in the present case is not affected by the principal motion, and so a precise probe of the extent of motion is lacking. The development of a detailed model of the intermolecular process seems difficult. The best approach including ^{1}H NMR line shape analysis would be to characterize the intramolecular motional contributions to narrowing as precisely as possible to separate out the effects of the intermolecular process for analysis.

Acknowledgment. Samples, dynamic mechanical data, and numerous discussions provided by Drs. J. T. Bendler and A. F. Yee, Research and Development Center, General Electric Corp., are greatly appreciated. We thank Mr. Francis Shea for assistance in the operation of the NMR spectrometer. The research was carried out with financial support of the National Science Foundation, Grant DMR-7906777, Polymers Program. This research was also supported in part by National Science Foundation Equipment Grant No. CHE 77-09059.

References and Notes

(1) Olf, A. G.; Peterlin, A. *J. Polym. Sci., Part A-2* **1970**, *8*, 753.
(2) Garfield, J. *J. Polym. Sci., Part C* **1970**, *30*, 551.
(3) Folkes, M. J.; Ward, I. M. *J. Mater. Sci.* **1971**, *6*, 582.
(4) Davenport, R. A.; Manuel, A. J. *Polymer* **1977**, *18*, 557.
(5) Van Vleck, J. H. *Phys. Rev.* **1948**, *74*, 1168.
(6) Andrew, E. R. "Nuclear Magnetic Resonance"; Cambridge University Press: New York, 1958; Chapter 6.
(7) Illers, K. H.; Breuer, H. *Kolloid Z. Z. Polym.* **1968**, *176* (2), 110.
(8) Le Grand, D. A.; Erhardt, P. F. *J. Appl. Polym. Sci.* **1969**, *13*, 1707.
(9) Lunn, A. C.; Lannas, L. V. *J. Polym. Sci., Polym. Phys. Ed.* **1972**, *10*, 2189.
(10) Schaefer, J.; Stejskal, E. O.; Buchdahl, R. *Macromolecules* **1977**, *10*, 384.
(11) Tonelli, E. *Macromolecules* **1972**, *5*, 558.
(12) Schatzki, T. *J. Polym. Sci.* **1962**, *57*, 496.
(13) Valeur, B.; Jarry, J. P.; Geny, F.; Monnerie, L. *J. Polym. Sci., Polym. Phys. Ed.* **1975**, *13*, 667.
(14) Jones, A. A.; Stockmayer, W. H. *J. Polym. Sci.* **1977**, *15*, 847.
(15) Pake, G. E. *J. Chem. Phys.* **1948**, *16*, 327.
(16) Andrew, E. R. *J. Chem. Phys.* **1950**, *18*, 607.
(17) Williams, A. D.; Flory, P. J. *J. Polym. Sci., Part A-2* **1968**, *6*, 1945.
(18) Hendrickson, J. R.; Bray, P. J. *J. Magn. Reson.* **1973**, *9*, 341.
(19) Yee, A. F.; Smith, S. A. *Macromolecules* **1981**, *14*, 54.
(20) Vandershaeren, J.; Linkens, A. *Macromolecules* **1978**, *11*, 1228.
(21) Jones, A. A.; Bisceglia, M. *Macromolecules* **1979**, *12*, 1136.
(22) VanderHart, D. L.; Gutowsky, H. S.; Farrar, T. C. *J. Am. Chem. Soc.* **1967**, *89*, 5056.

Rates of Conformational Transitions in Branched Chain Molecules

Jeffrey Skolnick* and Wayne L. Mattice

Department of Chemistry, Louisiana State University, Baton Rouge, Louisiana 70803.
Received September 2, 1980

ABSTRACT: A recently developed theory of the kinetics of conformational transitions based on a multidimensional extension of Kramers' rate theory is applied to branched polyethylene-like molecules. In particular, the influence of branching on the mechanism and rates of the trans → gauche transition is investigated. As in linear molecules, the reaction coordinate is a localized mode. Thus, the presence of an attached side chain introduces conformational rigidity into one of the tails connected to the transforming rotational angle, and the localized mode behaves akin to related linear molecules. In general, it is found that branches somewhat reduce the transition rate relative to the linear molecule; nevertheless the effect is fairly minor. Therefore, it is concluded that the time scale of conformational transitions in branched and linear chains is the same.

I. Introduction

The nature of local motions in polymers has been the object of considerable recent attention. Experiments have been designed to probe such molecular weight independent processes,[1-5] and computer simulations have given insight into kinetic properties of small-scale rearrangements in polymers.[6-10] These simulations provide a proving ground for various theoretical models of polymer dynamics, such as those of Fixman,[9] Fixman and Evans,[11] and Adler and Freed.[12] The mechanism of small-scale motions in linear chain molecules has been recently addressed.[13] We focus here on properties of a specific class of local motions (conformational transitions from one rotational isomeric state to another) in simple chains containing branches.

The approach used has its origin in a recent study[13] in which a multidimensional version of Kramers' reaction rate theory was formulated and applied to conformational transitions in linear molecules. Based on evidence extracted from experiment and computer simulations, the theory adopted the viewpoint that conformational changes occur via single, independent transition events. The method provided the capability of predicting the dependence of the transition rate, k, on chain geometry, size, solvent viscosity, and activation energy. The reaction coordinate in the vicinity of the barrier to conformational transitions (a saddle point in the multidimensional position phase

0024-9297/81/2214-0292$01.25/0 © 1981 American Chemical Society

space of the polymer) was analyzed in order to understand the behavior of the tails attached to the transforming bond. The reaction coordinate was found to be a localized mode in the sense that the attached tails distort to maximize rotation about the transforming bond. Moreover, the motion of the tails diminishes with increasing distance from the reaction center. Comparison of calculated values of k with those found in Brownian dynamics simulations[7] revealed good qualitative and fair quantitative agreement.

While some polymers can be modeled as flexible linear molecules, most polymers possess side chains and/or branched main chains. In the latter case a polymer molecule may possess more than two ends. The question naturally arises as to the influence of branched tails on the motion of the bond undergoing the conformational transition. Does the extra "tail" behave akin to a "rigid" conformation in linear molecules? In this case, the localized mode will distort out the more flexible end and should give essentially the same transition rates as the linear molecule. On the other hand, branched tails might exert such a large frictional resistance that conformational transition rates are drastically reduced relative to that in linear molecules. In the context of the multidimensional Kramers reaction rate theory, we shall develop a qualitative picture of the effect of chain branching on conformational transitions.

We have chosen a polyethylene-like molecule for study. One of the reasons for the commercial importance of polyethylene is its versatility, arising from the fact that different physical properties can be obtained, depending on the reaction conditions employed for its preparation. Among the factors affecting its physical properties is the presence of short branches, which exert a strong influence on morphology and solid-state properties of low-density polyethylene. Recent careful ^{13}C nuclear magnetic resonance studies convincingly demonstrate that the number and type of short branches vary dramatically from one sample of low-density polyethylene to another.[14] Butyl branches are commonly found to be present.[14-19] Additional types of short branches include 1,3-paired diethyl, amyl, and 2-ethylhexyl, as well as others not yet identified.[14] It is well-known that branches produce a substantial alteration in the dimensions.[20-24] and asymmetry[25-27] of the isolated, unperturbed polyethylene molecule. Due to the complexity of the potential energy surface, we cannot at this point hope to provide a quantitative estimate of the transition rate in real polyethylene; we can, however, in the context of a model provide a qualitative answer to the question: Does the presence of branches alter the rate of trans to gauche transitions in unperturbed polyethylene-like molecules?

This work treats a branched alkane-like molecule containing 16 main-chain vertices, and a side chain having up to 7 vertices. As previously,[13] each vertex represents a carbon atom and substituent hydrogens. The molecule is treated in the rotational isomeric state approximation. Torsional, angle bending, and bond stretching potentials are identical with those used in the linear alkane calculation. A 16-vertex main chain is chosen because in linear molecules it reveals all the qualitative features of the polymer localized mode. We shall calculate the transition rate of the central torsional angle in the main chain as a function of the position, size, and conformation of an attached branch.

II. Molecular Model: Chain Potential

Consider a chain molecule in which the only allowed interactions along the backbone are of the bond stretching, angle bending, and independent torsional potential variety. In the current treatment, neither excluded-volume effects nor hydrodynamic interactions are permitted. On the distance and time scales of conformational transitions, these approximations are fairly reasonable.

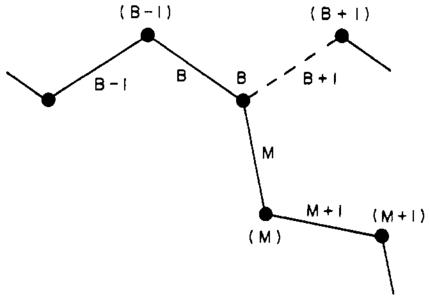

Figure 1. Labeling of the vertices in the vicinity of an attached branch.

Let the branched chain molecule consist of M_T identical vertices, where, as usual, each vertex represents a carbon atom with its substituent hydrogens. The main chain consists of M vertices indexed 0 to $M - 1$. A branch is joined to the main chain at vertex B. Thus the branch contains $M_T - M$ vertices indexed M to $M_T - 1$. This indexing scheme is depicted in Figure 1.

Bonds in the branched molecule are assumed to experience the same bond stretching, bond angle bending, and torsional potentials as those used to treat transition rates in unbranched alkanes.[13] Interdependence of rotations about adjacent bonds is ignored. Since independent rotations are assumed for both linear and branched molecules, this oversimplification should be of little consequence for the *ratio* of the computed transition rates. A further assumption is additivity of first-order interactions at bonds connected to the atom at the branch point. While this assumption cannot be rigorously justified,[28] its use does not alter the qualitative conclusions reached in this study; we return to this point later.

The bonds in the molecule experience a potential $V_b(b_i)$ that is harmonic in the difference between the bond length $|\mathbf{b}_i|$ and a value b_0

$$V_b(b_i) = \frac{\gamma_b}{2}\left(|\mathbf{b}_i| - b_0\right)^2 \qquad \text{(II.1)}$$

γ_b is the bond stretching force constant.

The bond angles θ_i located between bonds i and $i + 1$ are held near the tetrahedral value θ_0 by

$$V_\theta(\theta_i) = \frac{\gamma_\theta}{2}(\cos\theta_i - \cos\theta_0)^2 \qquad \text{(II.2)}$$

γ_θ is the angle bending force constant.

Bond rotation is characterized by a torsional angle ϕ_i defined by the dihedral angle between the plane of bond $i - 1$ and i and i and $i + 1$. The torsional potential is

$$V_\phi(\phi_i) = \gamma_\phi \sum_{n=0}^{5} a_n \cos^n \phi_i \qquad \text{(II.3)}$$

γ_ϕ is the torsional force constant. The zero of the torsional potential is the trans state where $\phi_i = 0$.

In the spirit of reaction rate theory we shall require the behavior of the torsional potential in the neighborhood of the initial state well and the barrier. Near the trans state

$$V_\phi(\phi_i) = \frac{\gamma_t}{2}\phi_i^2 \qquad \text{(II.4)}$$

Near a gauche state situated at ϕ_g (the potential is symmetric)

$$V_\phi(\phi_i) = E_g + \frac{\gamma_g}{2}(\phi_i - \phi_g)^2 \qquad \text{(II.5)}$$

In the vicinity of the trans–gauche barrier located at ϕ^*

$$V_\phi(\phi_i) = E^* - \frac{\gamma^*}{2}(\phi_i - \phi^*)^2 \qquad \text{(II.6)}$$

The form of the potential is reminiscent of that in alkanes. To make contact with previous work on linear chain molecules, we have employed the same parameters used in paper 1.[13]

The total bond stretching potential, V_b, is composed of the bond stretching contributions of the main chain and those of the branch

$$V_b = \sum_{i=1}^{M-1} V_b(b_i) + \sum_{i=M}^{M_T-1} V_b(b_i) \qquad \text{(II.7)}$$

where bond M is located between vertex B and vertex M (see Figure 1).

In an analogous manner, the total angle bending potential is

$$V_\theta = \sum_{i=1}^{M-2} V_\theta(\theta_i) + \sum_{i=M-1}^{M_T-2} V_\theta(\theta_i) \qquad \text{(II.8)}$$

θ_{M-1} is the angle between bond B and bond M. Finally, the full torsional potential of the molecule, V_ϕ, is

$$V_\phi = \sum_{i=2}^{M-2} V_\phi(\phi_i) + \sum_{i=M-1}^{M_T-2} V_\phi(\phi_i) \qquad \text{(II.9)}$$

ϕ_{M-1} is the dihedral angle between the planes defined by bonds B and $B - 1$ and by bonds B and M.

Consequently, the total potential is

$$V_T = V_b + V_\theta + V_\phi \qquad \text{(II.10)}$$

with V_b, V_θ, and V_ϕ defined by eq II.7 to II.9.

In section IV, we shall justify the use of the forms of the potential used to construct V_T. Suffice it to say at this point that the incorporation of a more sophisticated potential that takes greater account of the presence of branching should not affect the qualitative conclusions of this study.

III. High-Friction Limit of Polymer Conformational Transitions

This section reviews the formulation of the high-friction limit of the multidimensional Kramers reaction rate theory.

When considering polymer conformational transitions, one has a multidimensional system. Let a particular bond i undergo the transition

$$\text{P-t-Q} \rightarrow \text{P}'\text{-g}^+\text{-Q}'$$

P and Q and P′ and Q′ denote the orientation of the tails before and after the conformational transition. The physical situation corresponds to that shown schematically in Figure 2. We want to calculate the rate of transition from a valley V to the valley V′ through a saddle point that is the center of the activated state. We now make the crucial assumption that there is only a single rotational barrier crossing associated with the conformational transition.

To proceed further, we recognize that the conformational transition rate is given by the flux through a plane containing the saddle point and which reasonably partitions the phase space into the two conformational states of bond i. The multidimensional calculation of the flux is quite analogous to the one-dimensional situation with the added features that (1) the reaction coordinate in the vicinity of the saddle point is the path of steepest descents from the saddle point and (2) the probability density, n^*, in the region of the saddle point is related to a free energy of activation; i.e., in addition to the activation energy, E^*, the entropy of activation representing the breadth of the pass must be included in n^*. All these conclusions can be rigorously shown from Blomberg's extension of the Kramers current conservation argument to multidimensional space.[29]

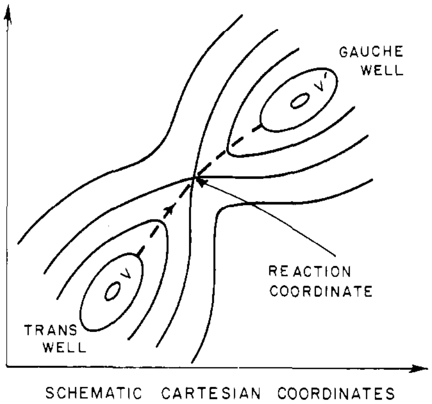

Figure 2. Schematic representation of the potential surface. The transition proceeds from the valley V to the valley V′ by passing in the vicinity of the saddle point.

Analogous to the one-dimensional treatment of Kramers[30] it is possible to show that the flux across the saddle point per polymer molecule in the well at V is given by

$$k = \frac{|\lambda|}{2\pi\zeta}\left(\frac{\gamma_t}{\gamma^*}\right)^{1/2} \exp\left\{\frac{-E^*}{k_B T}\right\} \qquad \text{(III.1)}$$

with γ_t and γ^* defined in eq II.4 and II.6, respectively. ζ is the friction constant per vertex, E^* is the barrier height of the transforming bond, and λ is the curvature of the path of steepest descents from the saddle point. For potentials of the type depicted in eq II.10, the influence of polymer tail size, orientation, and topology enters only in $|\lambda|$. The magnitude of $|\lambda|$ reflects the ability of a given tail orientation to maximize the rotation about the transforming bond. The more "flexible" the tail configurations are, the larger is the value of $|\lambda|$.

λ may be obtained by diagonalizing the potential interaction matrix **W** defined in the vicinity of the saddle point. The eigenvector ρ^*, whose negative eigenvalue is λ, points in the direction of the path of steepest descents from the barrier. A detailed discussion of the nature of the reaction coordinate may be found in Skolnick and Helfand.[13]

IV. Transitions in Branched Molecules

Representative rates for the t → g$^+$ transition of ϕ_8 have been computed for various chain configurations, branch size, and location. Before turning to an examination of the rates per se, it will prove useful to examine ρ^*, the localized mode over the barrier.

Much insight on the character of the transforming process can be gained from the localized mode over the barrier, ρ^*, if the vertex displacements are converted to torsional, angle bending, and bond stretching modes. We briefly review the technique for carrying out the transformations below.

Consider an overall motion of the polymer vertices $\{d\rho_i^*\}$ such that

$$\sum_{i=1}^{N} |\mathrm{d}\rho_i^{*2}| = b_0^2\,\mathrm{d}s^2 \qquad \text{(IV.1)}$$

Thus for a given total amount of motion bonds, the change in bond length of the ith bond is

$$\mathrm{d}b_i/b_0 = D_{b_i}\,\mathrm{d}s \qquad \text{(IV.2)}$$

Similarly, the change in the bond angle θ_i is

$$\mathrm{d}\theta_i = D_{\theta_i}\,\mathrm{d}s \quad \text{(radians)} \qquad \text{(IV.3)}$$

and the change in the ith torsional angle, ϕ_i, is

$$\mathrm{d}\phi_i = D_{\phi_i}\,\mathrm{d}s \quad \text{(radians)} \qquad \text{(IV.4)}$$

The explicit forms of D_{b_i}, D_{θ_i}, and D_{ϕ_i} may be found in Appendix C of ref 13.

In the following, a tail configuration is said to be more "flexible" in the direction of the reaction coordinate the larger the value of D_{ϕ_8} is relative to the other D_{ϕ_i}. Otherwise stated, for a given overall amount of motion, more "flexible" tails allow for increased distortion of the transforming rotational angle away from the saddle point; this produces an enhanced transition rate. "Rigid" tail configurations exhibit relatively smaller values of central angle torsional distortion. In general, these orientations require greater coupling into the angle bending and bond stretching degrees of freedom. As a consequence, the transition rate is smaller.

In all cases discussed below, the eigenvector, ρ^*, and its negative eigenvalue, λ, were determined numerically. The rate of conformational transition k was obtained from eq III.1. The barrier height E^* was taken to be $4k_BT$, and ζ was set equal to 1.4×10^3 kg/ns.[13]

Table I shows the torsional distortion, angle bending, and bond stretching associated with the reaction coordinate near the saddle point for

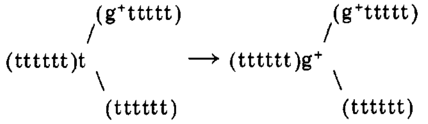

$$(\mathrm{tttttt})\mathrm{t}\begin{array}{l}\diagup(\mathrm{g^+tttt})\\ \\ \diagdown(\mathrm{tttttt})\end{array} \longrightarrow (\mathrm{tttttt})\mathrm{g^+}\begin{array}{l}\diagup(\mathrm{g^+tttt})\\ \\ \diagdown(\mathrm{tttttt})\end{array} \qquad \text{(IV.5)}$$

with $k = 2.59$ ns^{-1}. Furthermore, Table II presents the torsional, angle bending, and bond stretching modes for the localized mode in the transition

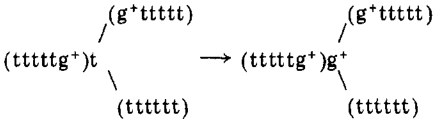

$$(\mathrm{tttttg^+})\mathrm{t}\begin{array}{l}\diagup(\mathrm{g^+tttt})\\ \\ \diagdown(\mathrm{tttttt})\end{array} \longrightarrow (\mathrm{tttttg^+})\mathrm{g^+}\begin{array}{l}\diagup(\mathrm{g^+tttt})\\ \\ \diagdown(\mathrm{tttttt})\end{array} \qquad \text{(IV.6)}$$

with $k = 0.46$ ns^{-1}.[31]

A study of Tables I and II and the localized mode of a host of other conformations not displayed here reveals these qualitative features of the reaction coordinate in branched molecules:

(A-1) The localized mode tends to distort away from the tail that possesses a branch. Thus, when a flexible nonbranched tail, e.g., (tttttt) is present, there is far greater distortion of the transforming angle ϕ_8 than when a rigid conformation, e.g., (tttttg$^+$) occurs. This is entirely consistent with the observations made on linear chain molecules. That is, one wants to maximize the motion of the transforming bond. The presence of additional vertices in the branch will tend to decrease the motion about ϕ_8. Consequently, the localized mode is somewhat shifted to the tail where fewer vertices are present.

(A-2) As in the case of linear chain molecules, the reaction coordinate couples most effectively into the softest degrees of freedom, the torsional modes.

Chart I

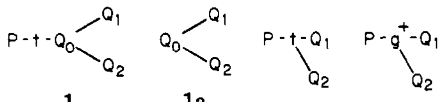

1 1a 2 3

(A-3) The torsional angle distortions occur so as to minimize the displacements of the vertices from the saddle point conformation.

(A-4) In short, the qualitative conclusions formulated for the reaction coordinate of linear molecules carry over to branched molecules, if the branched tail is viewed as a rigid conformation. Consequently, if the nonbranched tail is a rigid conformation, the distortion of ϕ_8 is small with a concomitantly low transition rate. (Exceptions to this rule are shown in Table III and discussed below.) On the other hand, if the nonbranched tail is flexible, significant displacement of ϕ_8 from the torsional potential maximum, ϕ_8^*, occurs and one expects a fast transition rate.

Tables III–VIII display representative values of k for the t → g$^+$ transition of ϕ_8 in various branched molecules. Transition rates of the nonbranched molecules are also tabulated. Let **1** (see Chart I) represent the initial state conformation of the branched molecule with tails P and Q_0Q_1 and Q_0Q_2. Q_0 is the configuration to the right of the transforming bond that is in common with tails Q_1 and Q_2. To quantitatively examine the influence of chain branching we shall compare the branched rate k_b with the rates of the linear molecules P-t-Q_0Q_1 and P-t-Q_0Q_2. P-t-Q_0Q_1 is called chain A and P-t-Q_0Q_2 is referred to as chain B where appropriate.

We have used a shorthand notation to describe the chain conformation in Tables III–VIII. For example (ttttg$^+$g$^+$) is represented by (t^{4}g^{+2}).

For all the conformations listed in Table III the branch is attached directly to the transforming bond rather than to a nontransforming bond in a tail. Schematically, the initial state conformation is **2** (Chart I) which transforms to **3** (Chart I). This situation is distinct from that encountered in Tables IV–VIII and is therefore treated separately.

An examination of the rates found in Table III leads to these observations:

(B-1) Branched molecule ϕ_8 transition rates are fairly close to those in the linear 16-vertex chain P-t-Q_1. The average of the ratios of the rates is 0.65 (standard deviations 0.14).

(B-2) Due to coupling through the torsional potential, the Q_2 branch acts to make the P rather than the Q_1 (see Tables I and II) branch behave like a rigid conformation. Thus the dominant effect on the transition rate is exerted by the Q_1 branch; i.e., if Q_1 is a flexible conformation, k_b is up to an order of magnitude larger than if Q_1 is rigid. Averages of the branched molecule rates in Table III (standard deviation in parentheses) are 3.04 (0.82) ns^{-1} if Q_1 is t^6 and 3.90 (0.79) ns^{-1} if Q_1 is tg$^+$t^4, but the average falls to only 0.96 (0.47) ns^{-1} if Q_1 is g$^+$t^5. In contrast, averages of branched molecule rates are 2.85 (1.37), 2.61 (0.54), and 2.98 (0.95) ns^{-1}, respectively, if Q_2 is t^6, g$^+$t^5, and tg$^+$t^4, showing the insensitivity of the rate of Q_2.

(B-3) Within a given rate range characteristic of Q_1, the transition rate will show the usual dependence on conformation in the P and Q_2 branch. Otherwise stated, if gauche bonds are even to the transforming

Table I. Localized mode for $(tttttt)t\langle^{(g^+ttttt)}_{(tttttt)}$ initial state, twenty-two vertex branched chain

$D_{\phi i}$ $i=8-j$	$D_{\phi i}$ $i=9+j$	$D_{\phi i}$ $i=14+j$	$D_{\theta i}$ $i=7-j$	$D_{\theta i}$ $i=9+j$	$D_{\theta i}$ $i=14+j$	D_{bi} $i=8-j$	D_{bi} $i=9+j$	D_{bi} $i=15+j$
1.17			−.030	−.14		−.11		
.16	−.080	.11	−.0041	.041	.050	−.0093	−.0074	−.0078
−.26	.11	−.11	−.021	−.043	−.052	−.0079	−.0045	−.0024
.061	−.055	.060	−.0038	.022	.020	−.0057	−.0012	−.0052
−.13	.050	−.053	−.011	−.019	−.020	−.0050	−.0035	−.0014
.0085	−.015	.018	−.0030	.0053	.0030	−.0032	−.00047	−.0023
−.047	.014	−.015	−.0042	−.0040	−.0044	−.0024	−.0017	−.00051
						−.0010	−.00016	

Table II. Localized mode for $(ttttg^+)t\langle^{(g^+ttttt)}_{(tttttt)}$ initial state twenty-two vertex branched chain.

j	$D_{\phi i}$ $i=8-j$	$D_{\phi i}$ $i=9+j$	$D_{\phi i}$ $i=14+j$	$D_{\theta i}$ $i=7-j$	$D_{\theta i}$ $i=9+j$	$D_{\theta i}$ $i=14+j$	D_{bi} $i=8-j$	D_{bi} $i=9+j$	D_{bi} $i=15+j$
0	.46			−.014	.000081		−.0011		
1	−.045	−.039	.017	.042	.038	−.012	−.00084	−.0015	−.00064
2	.052	.047	−.026	−.038	−.032	.0023	−.0034	−.0010	−.0015
3	−.037	−.034	.017	.025	.023	−.0033	.00019	.00045	−.00064
4	.027	.026	−.018	−.019	−.016	−.0014	−.0021	−.0013	−.00075
5	−.014	−.014	.0081	.086	.0082	−.00043	.00044	.00080	−.00043
6	.0077	.0076	−.0070	−.041	−.0032	−.0011	−.0012	−.00082	−.00021
7							.00031	.00032	

Table III. Representative rates of bond 8 t → g^+ chain transition in a 16 vertex chain, and a 23 vertex branched molecule with a seven vertex branch joined at vertex 8, $E^*/k_BT = 4$.

Initial State Chain Conformation	Rate ns^{-1}	Initial State Branched Molecule Conformation	Rate ns^{-1}
$(tttttt)t(tttttt)$	5.06	$(tttttt)t(tttttt)$ $g^-(tttttt)$	3.71
$(g^+ttttt)t(tttttt)$	4.67	$(g^+ttttt)t(tttttt)$ $g^-(tttttt)$	3.56
$(tg^+tttt)t(tttttt)$	4.09	$(tg^+tttt)t(tttttt)$ $g^-(tttttt)$	3.12
$(ttg^+ttt)t(tttttt)$	4.67	$(ttg^+ttt)t(tttttt)$ $g^-(tttttt)$	3.70
$(tttg^+tt)t(tttttt)$	3.48	$(tttg^+tt)t(tttttt)$ $g^-(tttttt)$	2.63
$(ttttg^+t)t(tttttt)$	6.54	$(ttttg^+t)t(tttttt)$ $g^-(tttttt)$	5.26
$(tttttg^+)t(tttttt)$	3.87	$(tttttg^+)t(tttttt)$ $g^-(tttttt)$	2.37
$(g^-ttttt)t(tttttt)$	4.61	$(g^-ttttt)t(tttttt)$ $g^-(tttttt)$	3.50
$(tg^-tttt)t(tttttt)$	4.21	$(tg^-tttt)t(tttttt)$ $g^-(tttttt)$	3.23
$(ttg^-ttt)t(tttttt)$	4.32	$(ttg^-ttt)t(tttttt)$ $g^-(tttttt)$	3.37
$(tttg^-tt)t(tttttt)$	3.57	$(tttg^-tt)t(tttttt)$ $g^-(tttttt)$	2.72
$(ttttg^-t)t(tttttt)$	4.81	$(ttttg^-t)t(tttttt)$ $g^-(tttttt)$	3.86
$(tttttg^-)t(tttttt)$	2.52	$(tttttg^-)t(tttttt)$ $g^-(tttttt)$	2.03
$(tttttt)t(g^+ttttt)$	3.87	$(tttttt)t(g^+ttttt)$ $g^-(tttttt)$	.98
$(g^+ttttt)t(g^+ttttt)$	3.11	$(g^+ttttt)t(g^+ttttt)$ $g^-(tttttt)$	1.03
$(tg^+tttt)t(g^+ttttt)$	1.98	$(tg^+tttt)t(g^+ttttt)$ $g^-(tttttt)$	.69
$(ttg^+ttt)t(g^+ttttt)$	2.57	$(ttg^+ttt)t(g^+ttttt)$ $g^-(tttttt)$	1.19
$(tttg^+tt)t(g^+ttttt)$	.93	$(tttg^+tt)t(g^+ttttt)$ $g^-(tttttt)$	.54
$(ttttg^+t)t(g^+ttttt)$	3.07	$(ttttg^+t)t(g^+ttttt)$ $g^-(tttttt)$	1.82
$(tttttg^+)t(g^+ttttt)$	.60	$(tttttg^+)t(g^+ttttt)$ $g^-(tttttt)$	.44
$(tttttt)t(tg^+tttt)$	6.54	$(tttttt)t(tg^+tttt)$ $g^-(tttttt)$	4.31
$(g^+ttttt)t(tg^+tttt)$	6.01	$(g^+ttttt)t(tg^+tttt)$ $g^-(tttttt)$	4.15
$(tg^+tttt)t(tg^+tttt)$	5.41	$(tg^+tttt)t(tg^+tttt)$ $g^-(tttttt)$	3.78
$(ttg^+ttt)t(tg^+tttt)$	5.72	$(ttg^+ttt)t(tg^+tttt)$ $g^-(tttttt)$	4.16
$(tttg^+tt)t(tg^+tttt)$	4.23	$(tttg^+tt)t(tg^+tttt)$ $g^-(tttttt)$	3.25
$(ttttg^+t)t(tg^+tttt)$	6.65	$(ttttg^+t)t(tg^+tttt)$ $g^-(tttttt)$	5.04
$(tttttg^+)t(tg^+tttt)$	3.07	$(tttttg^+)t(tg^+tttt)$ $g^-(tttttt)$	2.61
$(tttttt)t(tttttt)$	5.06	$(tttttt)t(tttttt)$ $g^-(tg^+tttt)$	3.40
$(g^+ttttt)t(tttttt)$	4.67	$(g^+ttttt)t(tttttt)$ $g^-(tg^+tttt)$	3.23
$(tg^+tttt)t(tttttt)$	4.09	$(tg^+tttt)t(tttttt)$ $g^-(tg^+tttt)$	2.69
$(ttg^+ttt)t(tttttt)$	4.67	$(ttg^+ttt)t(tttttt)$ $g^-(tg^+tttt)$	3.30
$(tttg^+tt)t(tttttt)$	3.48	$(tttg^+tt)t(tttttt)$ $g^-(tg^+tttt)$	2.09
$(ttttg^+t)t(tttttt)$	6.54	$(ttttg^+t)t(tttttt)$ $g^-(tg^+tttt)$	4.53
$(tttttg^+)t(tttttt)$	3.87	$(tttttg^+)t(tttttt)$ $g^-(tg^+tttt)$	1.54
$(tttttt)t(tttttt)$	5.06	$(tttttt)t(tttttt)$ $g^-(g^+ttttt)$	2.50
$(g^+ttttt)t(tttttt)$	4.67	$(g^+ttttt)t(tttttt)$ $g^-(g^+ttttt)$	2.49
$(tg^+tttt)t(tttttt)$	4.09	$(tg^+tttt)t(tttttt)$ $g^-(g^+ttttt)$	2.22
$(ttg^+ttt)t(tttttt)$	4.67	$(ttg^+ttt)t(tttttt)$ $g^-(g^+ttttt)$	2.69
$(tttg^+tt)t(tttttt)$	3.48	$(tttg^+tt)t(tttttt)$ $g^-(g^+ttttt)$	2.14
$(ttttg^+t)t(tttttt)$	6.54	$(ttttg^+t)t(tttttt)$ $g^-(g^+ttttt)$	3.77
$(tttttg^+)t(tttttt)$	3.87	$(tttttg^+)t(tttttt)$ $g^-(g^+ttttt)$	2.44

e IV. Representative rates of bond 8 t → g^+ transition in a 16 vertex chain A, sixteen vertex chain B, and the 22 vertex branched molecule containing a six vertex branch attached to vertex 9, $E^*/k_BT = 4$.

ial State n A ormation	Rate ns^{-1}	Initial State Chain B Conformation	Rate ns^{-1}	Initial State Branched Molecule Conformation	Rate ns^{-1}
$t(g^+t^5)$	3.88	$(t^6)t(t^6)$	5.06	$t^6t-(g^+t^5)$ (t^6)	2.59
$^5)t(g^+t^5)$	3.11	$(g^+t^5)t(t^6)$	4.57	$(g^+t^5)t-(g^+t^5)$ (t^6)	2.16
$^4)t(g^+t^5)$	1.95	$(tg^+t^4)t(t^6)$	4.09	$(tg^+t^4)t-(g^+t^5)$ (t^6)	1.20
$^+t^3)t(g^+t^5)$	2.57	$(t^2g^+t^3)t(t^6)$	4.67	$(t^2g^+t^3)t-(g^+t^5)$ (t^6)	1.99
$^+t^2)t(g^+t^5)$	.93	$(t^3g^+t^2)t(t^6)$	3.49	$(t^3g^+t^2)t-(g^+t^5)$ (t^6)	.65
$^+t)t(g^+t^5)$	3.08	$(t^4g^+t)t(t^6)$	6.54	$(t^4g^+t)t-(g^+t^5)$ (t^6)	2.71
$^+)t(g^+t^5)$	.60	$(t^5g^+)t(t^6)$	3.38	$(t^5g^+)t-(g^+t^5)$ (t^6)	.46
$^5)t(g^+t^5)$	3.11	$(g^+t^5)t(tg^+t^4)$	6.01	$(g^+t^5)t-(g^+t^5)$ (tg^+t^4)	2.77
$^4)t(g^+t^5)$	1.98	$(tg^+t^4)t(tg^+t^4)$	5.41	$(tg^+t^4)t-(g^+t^5)$ (tg^+t^4)	1.73
$^+t^3)t(g^+t^5)$	2.57	$(t^2g^+t^3)t(tg^+t^4)$	5.72	$(t^2g^+t^3)t-(g^+t^5)$ (tg^+t^4)	2.39
$^+t^2)t(g^+t^5)$	.93	$(t^3g^+t^2)t(tg^+t^4)$	4.23	$(t^3g^+t^2)t-(g^+t^5)$ (tg^+t^4)	.85
$^+t)t(g^+t^5)$	3.08	$(t^4g^+t)t(tg^+t^4)$	6.65	$(t^4g^+t)t-(g^+t^5)$ (tg^+t^4)	2.72
$^+)t(g^+t^5)$	.60	$(t^5g^+)t(tg^+t^4)$	3.05	$(t^5g^+)t-(g^+t^5)$ (tg^+t^4)	.49
$^3)t(g^+t^4g^+)$	2.54	$(t^2g^+t^3)t(t^5g^-)$	4.19	$(t^2g^+t^3)t-(g^+t^4g^+)$ (t^5g^-)	2.00
$t^3)t(g^+t^3g^+t)$	2.49	$(t^2g^+t^3)t(t^5g^-)$	4.19	$(t^2g^+t^3)t-(g^+t^3g^+t)$ (t^5g^-)	1.98
$^3)t(g^+t^2g^+t^2)$	2.57	$(t^2g^+t^3)t(t^5g^-)$	4.19	$(t^2g^+t^3)t-(g^+t^2g^+t^2)$ (t^5g^-)	2.04
$^3)t(g^+tg^+t^3)$	2.43	$(t^2g^+t^3)t(t^5g^-)$	4.19	$(t^2g^+t^3)t-(g^+tg^+t^3)$ (t^5g^-)	1.97
$^+t^3)t(g^{+2}t^4)$	2.89	$(t^2g^+t^3)t(t^5g^-)$	4.19	$(t^2g^+t^3)t-(g^{+2}t^4)$ (t^5g^-)	2.13
$^+t^3)t(g^+t^5)$	2.57	$(t^2g^+t^3)t(g^-g^+t^4)$	2.49	$(t^2g^+t^3)t-(g^+t^5)$ $(g^-g^+t^4)$	1.61
$^5)t(g^+t^5)$	3.11	$(g^+t^5)t(t^2g^+t^3)$	2.97	$(g^+t^5)t-(g^+t^5)$ $(t^2g^+t^3)$	2.21
$^4)t(g^+t^5)$	1.98	$(tg^+t^4)t(t^2g^+t^3)$	1.92	$(tg^+t^4)t-(g^+t^5)$ $(t^2g^+t^3)$	1.23
$^+t^3)t(g^+t^5)$	2.57	$(t^2g^+t^3)t(t^2g^+t^3)$	2.83	$(t^2g^+t^3)t-(g^+t^5)$ $(t^2g^+t^3)$	1.94
$^+t^3)t(t^4g^-t)$	3.69	$(t^2g^+t^3)t(g^+t^4g^-)$	2.59	$(t^2g^+t^3)t-(t^4g^-t)$ $(g^+t^4g^-)$	1.96
$^+t^3)t(t^3g^-t^2)$	3.89	$(t^2g^+t^3)t(g^+t^4g^-)$	2.59	$(t^2g^+t^3)t-(t^3g^-t^2)$ $(g^+t^4g^-)$	2.07
$^+t^3)t(t^2g^-t^3)$	2.94	$(t^2g^+t^3)t(g^+t^4g^-)$	2.59	$(t^2g^+t^3)t-(t^2g^-t^3)$ $(g^+t^4g^-)$	1.88
$^+t^3)t(tg^-t^4)$	4.34	$(t^2g^+t^3)t(g^+t^4g^-)$	2.59	$(t^2g^+t^3)t-(tg^-t^4)$ $(g^+t^4g^-)$	2.14
$^5)t(t^6)$	4.67	$(g^+t^5)t(g^+tg^+t^3)$	2.78	$(g^+t^5)t(t^6)$ $(g^+tg^+t^3)$	2.08
$^4)t(t^6)$	4.09	$(tg^+t^4)t(g^+tg^+t^3)$	1.68	$(tg^+t^4)t(t^6)$ $(g^+tg^+t^3)$	1.14

Table V. Representative rates of bond 8 t → g^+ transition in a sixteen vertex chain A, 12 vertex chain B, and the 17 vertex branched molecule containing a one vertex branch located at vertex 10, $E^*/k_BT = 4$.

Initial State, Chain A Conformation	Rate ns^{-1}	Initial State, Chain B Conformation	Rate ns^{-1}	Initial State, Branched Molecule Conformation	Rate ns^{-1}
$(t^6)t(tg^+t^4)$	6.54	$(t^6)t(t^2)$	6.21	$(t^6)t(tg^+t^4)$ t	4.17
$(g^+t^5)t(tg^+t^4)$	6.01	$(g^+t^5)t(t^2)$	5.88	$(g^+t^5)t(tg^+t^4)$ t	3.69
$(tg^+t^4)t(tg^+t^4)$	5.41	$(tg^+t^4)t(t^2)$	5.47	$(tg^+t^4)t(tg^+t^4)$ t	2.95
$(t^2g^+t^3)t(tg^+t^4)$	5.72	$(t^2g^+t^3)t(t^2)$	5.88	$(t^2g^+t^3)t(tg^+t^4)$ t	3.47
$(t^3g^+t^2)t(tg^+t^4)$	4.23	$(t^3g^+t^2)t(t^2)$	4.91	$(t^3g^+t^2)t(tg^+t^4)$ t	2.07
$(t^4g^+t)t(tg^+t^4)$	6.65	$(t^4g^+t)t(t^2)$	7.73	$(t^4g^+t)t(tg^+t^4)$ t	4.31
$(t^5g^+)t(tg^+t^4)$	3.07	$(t^5g^+)t(t^2)$	5.45	$(t^5g^+)t(tg^+t^4)$ t	1.45
$(g^-t^5)t(tg^+t^4)$	5.98	$(g^-t^5)t(t^2)$	5.84	$(g^-t^5)t(tg^+t^4)$ t	3.65
$(tg^-t^4)t(tg^+t^4)$	5.50	$(tg^-t^4)t(t^2)$	5.56	$(tg^-t^4)t(tg^+t^4)$ t	3.03
$(t^2g^-t^3)t(tg^+t^4)$	5.51	$(t^2g^-t^3)t(t^2)$	5.57	$(t^2g^-t^3)t(tg^+t^4)$ t	3.29
$(t^3g^-t^2)t(tg^+t^4)$	4.41	$(t^3g^-t^2)t(t^2)$	4.99	$(t^3g^-t^2)t(tg^+t^4)$ t	2.17
$(t^4g^-t)t(tg^+t^4)$	5.56	$(t^4g^-t)t(t^2)$	5.99	$(t^4g^-t)t(tg^+t^4)$ t	3.53
$(t^5g^-)t(tg^+t^4)$	2.99	$(t^5g^-)t(t^2)$	4.18	$(t^5g^-)t(tg^+t^4)$ t	1.35
$(g^+t^5)t(g^{+2}t^4)$	3.32	$(g^+t^5)t(g^+t)$	3.72	$(g^+t^5)t(g^+g^+t^4)$ t	2.79
$(tg^+t^4)t(g^{+2}t^4)$	2.26	$(tg^+t^4)t(g^+t)$	2.81	$(tg^+t^4)t(g^+g^+t^4)$ t	1.82
$(t^2g^+t^3)t(g^{+2}t^4)$	2.89	$(t^2g^+t^3)t(g^+t)$	3.38	$(t^2g^+t^3)t(g^+g^+t^4)$ t	2.49
$(t^3g^+t^2)t(g^{+2}t^4)$	1.15	$(t^3g^+t^2)t(g^+t)$	1.97	$(t^3g^+t^2)t(g^+g^+t^4)$ t	.98
$(t^4g^+t)t(g^{+2}t^4)$	3.48	$(t^4g^+t)t(g^+t)$	4.11	$(t^4g^+t)t(g^+g^+t^4)$ t	3.14
$(t^5g^+)t(g^{+2}t^4)$	.70	$(t^5g^+)t(g^+t)$	1.78	$(t^5g^+)t(g^+g^+t^4)$ t	.64
$(t^6)t(g^{+2}t^4)$	4.00	$(t^6)t(g^+t)$	4.36	$(t^6)t(g^+g^+t^4)$ t	3.34
$(t^6)t(tg^{+2}t^3)$	4.63	$(t^6)t(t^2)$	6.21	$(t^6)t(tg^{+2}t^3)$ t	3.43
$(g^+t^5)t(tg^{+2}t^3)$	3.98	$(g^+t^5)t(t^2)$	5.88	$(g^+t^5)t(tg^{+2}t^3)$ t	2.91
$(tg^+t^4)t(tg^{+2}t^3)$	3.04	$(tg^+t^4)t(t^2)$	5.47	$(tg^+t^4)t(tg^{+2}t^3)$ t	2.00
$(t^2g^+t^3)t(tg^{+2}t^3)$	3.61	$(t^2g^+t^3)t(t^2)$	5.88	$(t^2g^+t^3)t(tg^{+2}t^3)$ t	2.65
$(t^3g^+t^2)t(tg^{+2}t^3)$	1.65	$(t^3g^+t^2)t(t^2)$	4.91	$(t^3g^+t^2)t(tg^{+2}t^3)$ t	1.07
$(t^4g^+t)t(tg^{+2}t^3)$	4.61	$(t^4g^+t)t(t^2)$	7.73	$(t^4g^+t)t(tg^{+2}t^3)$ t	3.53
$(t^5g^+)t(tg^{+2}t^3)$	.76	$(t^5g^+)t(t^2)$	5.45	$(t^5g^+)t(tg^{+2}t^3)$ t	.57
$(g^+t^5)t(g^{+2}t^4)$	3.32	$(g^+t^5)t(g^+g^-)$	5.43	$(g^+t^5)t(g^+g^+t^4)$ g^-	3.00
$(tg^+t^4)t(g^{+2}t^4)$	2.26	$(tg^+t^4)t(g^+g^-)$	4.61	$(tg^+t^4)t(g^+g^+t^4)$ g^-	2.00
$(t^2g^+t^3)t(g^{+2}t^4)$	2.89	$(t^2g^+t^3)t(g^+g^-)$	5.02	$(t^2g^+t^3)t(g^+g^+t^4)$ g^-	2.67
$(t^3g^+t^2)t(g^{+2}t^4)$	1.15	$(t^3g^+t^2)t(g^+g^-)$	3.39	$(t^3g^+t^2)t(g^+g^+t^4)$ g^-	1.06
$(t^4g^+t)t(g^{+2}t^4)$	3.48	$(t^4g^+t)t(g^+g^-)$	5.52	$(t^4g^+t)t(g^+g^+t^4)$ g^-	3.33
$(t^5g^+)t(g^{+2}t^4)$	.70	$(t^5g^+)t(g^+g^-)$	2.72	$(t^5g^+)t(g^+g^+t^4)$ g^-	.68

bond, the configuration is more flexible and the rates are larger. Analogously, if the gauche bonds occur at an odd position to bond 8, the conformation is more rigid and k_b is smaller.

The analysis of the angle bending, torsional, and bond stretching contributions leads to the same qualitative conclusions for molecules of type **2** with P viewed as a "rigid" conformation as that found for **1** with **1a** the "rigid" conformation. (Examples of the latter are found in Tables I and II.) Thus, no explicit presentation of the former kind of localized mode is made.

It can be argued that for molecules of type **2**, the torsional potential we have employed neglects the direct torsional coupling between Q_1 and Q_2; consequently, the rigidity of the P conformation is overemphasized relative to that of Q_1. While this is certainly true, nevertheless even when P, Q_1, and Q_2 are *all* rigid tails, the transition rate is the same order of magnitude as that in a typical linear molecule. Thus, the qualitative conclusion (B-1) that transition rates are quite near those in linear molecules

Table VI. Representative rates of bond 6 t → g^+ transition in a 16 vertex chain A, 16 vertex chain B, and the 21 vertex branched molecule containing a 5 vertex branch attached at vertex 10, $E^*/k_BT = 4$.

Initial State, Chain A Conformation	Rate ns^{-1}	Initial State, Chain B Conformation	Rate ns^{-1}	Initial State Branched Molecule Conformation	Rate ns^{-1}
$(t^6)t(tg^+t^4)$	6.54	$(t^6)t(t^6)$	5.06	$(t^6)t(tg^+t^4)$ (t^5)	3.15
$(g^+t^5)t(tg^+t^4)$	6.01	$(g^+t^5)t(t^6)$	4.67	$(g^+t^5)t(tg^+t^4)$ (t^5)	2.67
$(tg^+t^4)t(tg^+t^4)$	5.41	$(tg^+t^4)t(t^6)$	4.09	$(tg^+t^4)t(tg^+t^4)$ (t^5)	1.77
$(t^2g^+t^3)t(tg^+t^4)$	5.72	$(t^2g^+t^3)t(t^6)$	4.67	$(t^2g^+t^3)t(tg^+t^4)$ (t^5)	2.45
$(t^3g^+t^2)t(tg^+t^4)$	4.23	$(t^3g^+t^2)t(t^6)$	3.48	$(t^3g^+t^2)t(tg^+t^4)$ (t^5)	.88
$(t^4g^+t)t(tg^+t^4)$	6.65	$(t^4g^+t)t(t^6)$	6.54	$(t^4g^+t)t(tg^+t^4)$ (t^5)	2.41
$(t^5g^+)t(tg^+t^4)$	6.54	$(t^5g^+)t(t^6)$	3.88	$(t^5g^+)t(tg^+t^4)$ (t^5)	.53
$(t^6)t(g^{+2}t^4)$	4.01	$(t^6)t(g^+t^5)$	3.88	$(t^6)t(g^+g^+t^4)$ (t^5)	2.87
$(g^+t^5)t(g^{+2}t^4)$	3.32	$(g^+t^5)t(g^+t^5)$	3.11	$(g^+t^5)t(g^+g^+t^4)$ (t^5)	2.33
$(tg^+t^4)t(g^{+2}t^4)$	2.26	$(tg^+t^4)t(g^+t^5)$	1.98	$(tg^+t^4)t(g^+g^+t^4)$ (t^5)	1.32
$(t^2g^+t^3)t(g^{+2}t^4)$	2.69	$(t^2g^+t^3)t(g^+t^5)$	2.57	$(t^2g^+t^3)t(g^+g^+t^4)$ (t^5)	2.05
$(t^3g^+t^2)t(g^{+2}t^4)$	1.15	$(t^3g^+t^2)t(g^+t^5)$	.92	$(t^3g^+t^2)t(g^+g^+t^4)$ (t^5)	.64
$(t^4g^+t)t(g^{+2}t^4)$	3.48	$(t^4g^+t)t(g^+t^5)$	3.08	$(t^4g^+t)t(g^+g^+t^4)$ (t^5)	2.69
$(t^5g^+)t(g^{+2}t^4)$	.70	$(t^5g^+)t(g^+t^5)$	.60	$(t^5g^+)t(g^+g^+t^4)$ (t^5)	.41
$(g^+t^5)t(g^{+2}t^4)$	3.32	$(g^+t^5)t(g^+tg^+t^3)$	2.78	$(g^+t^5)t(g^+g^+t^4)$ (tg^+t^3)	2.23
$(t^2g^+t^3)t(g^{+2}t^4)$	2.89	$(t^2g^+t^3)t(g^+tg^+t^3)$	2.47	$(t^2g^+t^3)t(g^+g^+t^4)$ (tg^+t^3)	2.00
$(t^3g^+t^2)t(g^{+2}t^4)$	1.15	$(t^3g^+t^2)t(g^+tg^+t^3)$	.84	$(t^3g^+t^2)t(g^+g^+t^4)$ (tg^+t^3)	.57
$(t^4g^+t)t(g^{+2}t^4)$	3.48	$(t^4g^+t)t(g^+tg^+t^3)$	3.14	$(t^4g^+t)t(g^+g^+t^4)$ (tg^+t^3)	2.70
$(t^5g^+)t(g^{+2}t^4)$	.70	$(t^5g^+)t(g^+tg^+t^3)$	.58	$(t^5g^+)t(g^+g^+t^4)$ (tg^+t^3)	.35
$(t^6)t(g^{+2}t^4)$	4.01	$(t^6)t(g^+tg^+t^3)$	3.42	$(t^6)t(g^+g^+t^4)$ (tg^+t^3)	2.72
$(g^+t^3g^+t)t(g^{+2}t^4)$	3.24	$(g^+t^3g^+t)t(g^+t^5)$	2.84	$(g^+t^3g^+t)t(g^+g^+t^4)$ (t^5)	1.51

Table VII. Representative rates of bond 8 t → g^+ transition in a 16 vertex chain A, 16 vertex chain B, and a 20 vertex branched molecule containing a 4 vertex branch attached to vertex 11, $E^*/k_BT = 4$.

Initial State, Chain A Conformation	Rate ns^{-1}	Initial State, Chain B Conformation	Rate ns^{-1}	Initial State, Branched Molecule Conformation	Rate ns^{-1}
$(t^6)t(t^2g^+t^3)$	3.48	$(t^6)t(t^6)$	5.06	$(t^6)t(t^2g^+t^3)$ (t^4)	3.32
$(g^+t^5)t(t^2g^+t^3)$	2.97	$(g^+t^5)t(t^6)$	4.67	$(g^+t^5)t(t^2g^+t^3)$ (t^4)	2.52
$(tg^+t^4)t(t^2g^+t^3)$	1.92	$(tg^+t^4)t(t^6)$	4.09	$(tg^+t^4)t(t^2g^+t^3)$ (t^4)	1.77
$(t^2g^+t^3)t(t^2g^+t^3)$	2.83	$(t^2g^+t^3)t(t^6)$	4.67	$(t^2g^+t^3)t(t^2g^+t^3)$ (t^4)	2.72
$(t^3g^+t^2)t(t^2g^+t^3)$	1.12	$(t^3g^+t^2)t(t^6)$	3.48	$(t^3g^+t^2)t(t^2g^+t^3)$ (t^4)	1.03
$(t^4g^+t)t(t^2g^+t^3)$	4.23	$(t^4g^+t)t(t^6)$	6.54	$(t^4g^+t)t(t^2g^+t^3)$ (t^4)	4.11
$(t^5g^+)t(t^2g^+t^3)$	.93	$(t^5g^+)t(t^6)$	3.88	$(t^5g^+)t(t^2g^+t^3)$ (t^4)	.81
$(g^+t^5)t(t^2g^+t^3)$	2.97	$(g^+t^5)t(t^3g^+t^2)$	4.25	$(g^+t^5)t(t^2g^+t^3)$ (tg^+t^2)	2.87
$(tg^+t^4)t(t^2g^+t^3)$	1.92	$(tg^+t^4)t(t^3g^+t^2)$	3.57	$(tg^+t^4)t(t^2g^+t^3)$ (tg^+t^2)	1.83
$(t^2g^+t^3)t(t^2g^+t^3)$	2.83	$(t^2g^+t^3)t(t^3g^+t^2)$	4.18	$(t^2g^+t^3)t(t^2g^+t^3)$ (tg^+t^2)	2.73
$(t^3g^+t^2)t(t^2g^+t^3)$	1.12	$(t^3g^+t^2)t(t^3g^+t^2)$	2.83	$(t^3g^+t^2)t(t^2g^+t^3)$ (tg^+t^2)	1.03
$(t^4g^+t)t(t^2g^+t^3)$	4.23	$(t^4g^+t)t(t^3g^+t^2)$	5.72	$(t^4g^+t)t(t^2g^+t^3)$ (tg^+t^2)	4.01
$(t^5g^+)t(t^2g^+t^3)$	.93	$(t^5g^+)t(t^3g^+t^2)$	2.57	$(t^5g^+)t(t^2g^+t^3)$ (tg^+t^2)	.71
$(t^6)t(t^2g^+t^3)$	3.48	$(t^6)t(t^3g^+t^2)$	4.67	$(t^6)t(t^2g^+t^3)$ (tg^+t^2)	3.36
$(t^6)t(g^+tg^+t^3)$	3.41	$(t^6)t(g^+t^2g^+t^2)$	3.68	$(t^6)t(g^+tg^+t^3)$ (tg^+t^2)	3.26
$(t^6)t(t^2g^{+2}t^2)$	3.52	$(t^6)t(t^6)$	5.05	$(t^6)t(t^2g^{+2}t^2)$ (t^4)	3.36
$(g^+t^5)t(t^2g^{+2}t^2)$	3.05	$(g^+t^5)t(t^6)$	4.67	$(g^+t^5)t(t^2g^{+2}t^2)$ (t^4)	2 88
$(tg^+t^4)t(t^2g^{+2}t^2)$	2.08	$(tg^+t^4)t(t^6)$	4.09	$(tg^+t^4)t(t^2g^{+2}t^2)$ (t^4)	1.88
$(t^2g^+t^3)t(t^2g^{+2}t^2)$	2.95	$(t^2g^+t^3)t(t^6)$	4.67	$(t^2g^+t^3)t(t^2g^{+2}t^2)$ (t^4)	2.79
$(t^3g^+t^2)t(t^2g^{+2}t^2)$	1.34	$(t^3g^+t^2)t(t^6)$	3.48	$(t^3g^+t^2)t(t^2g^{+2}t^2)$ (t^4)	1.17
$(t^4g^+t)t(t^2g^{+2}t^2)$	4.32	$(t^4g^+t)t(t^6)$	6.54	$(t^4g^+t)t(t^2g^{+2}t^2)$ (t^4)	4.17
$(t^5g^+)t(t^2g^{+2}t^2)$	1.14	$(t^5g^+)t(t^6)$	3.88	$(t^5g^+)t(t^2g^{+2}t^2)$ (t^4)	.94
$(t^6)t(tg^{+3}t^2)$	4.45	$(t^6)t(tg^+t^4)$	6.54	$(t^6)t(tg^+g^{+2}t^2)$ (t^4)	4.04

Table VIII. Representative rate of bond 6 t → g^+ transition in a 16 vertex chain A, 16 vertex chain B, and a 19 vertex branched molecule containing a 3 vertex branch attached at vertex 12, $E^*/k_BT = 4$.

Initial State, Chain A Conformation	Rate ns^{-1}	Initial State, Chain B Conformation	Rate ns^{-1}	Initial State, Branched Molecule Conformation	Rate ns^{-1}
$(t^6)t(t^3g^+t^2)$	4.67	$(t^6)t(t^6)$	5.06	$(t^6)t(t^3g^+t^2)$ (t^3)	3.87
$(g^+t^5)t(t^3g^+t^2)$	4.25	$(g^+t^5)t(t^6)$	4.67	$(g^+t^5)t(t^3g^+t^2)$ (t^3)	3.37
$(tg^+t^4)t(t^3g^+t^2)$	3.57	$(tg^+t^4)t(t^6)$	4.09	$(tg^+t^4)t(t^3g^+t^2)$ (t^3)	2.46
$(t^2g^+t^3)t(t^3g^+t^2)$	4.18	$(t^2g^+t^3)t(t^6)$	4.67	$(t^2g^+t^3)t(t^3g^+t^2)$ (t^3)	3.27
$(t^3g^+t^2)t(t^3g^+t^2)$	2.83	$(t^3g^+t^2)t(t^6)$	3.48	$(t^3g^+t^2)t(t^3g^+t^2)$ (t^3)	1.61
$(t^4g^+t)t(t^3g^+t^2)$	5.72	$(t^4g^+t)t(t^6)$	6.54	$(t^4g^+t)t(t^3g^+t^2)$ (t^3)	4.81
$(t^5g^+)t(t^3g^+t^2)$	2.57	$(t^5g^+)t(t^6)$	3.88	$(t^5g^+)t(t^3g^+t^2)$ (t^3)	1.30
$(t^6)t(t^3g^+t^2)$	4.67	$(t^6)t(t^4g^+t)$	4.09	$(t^6)t(t^3g^+t^2)$ (tg^+t)	3.65
$(g^+t^5)t(t^3g^+t^2)$	4.25	$(g^+t^5)t(t^4g^+t)$	3.61	$(g^+t^5)t(t^3g^+t^2)$ (tg^+t)	3.14
$(tg^+t^4)t(t^3g^+t^2)$	3.57	$(tg^+t^4)t(t^4g^+t)$	2.70	$(tg^+t^4)t(t^3g^+t^2)$ (tg^+t)	2.15
$(t^2g^+t^3)t(t^3g^+t^2)$	4.18	$(t^2g^+t^3)t(t^4g^+t)$	3.57	$(t^2g^+t^3)t(t^3g^+t^2)$ (tg^+t)	3.03
$(t^3g^+t^2)t(t^3g^+t^2)$	2.83	$(t^3g^+t^2)t(t^4g^+t)$	1.92	$(t^3g^+t^2)t(t^3g^+t^2)$ (tg^+t)	1.29
$(t^4g^+t)t(t^3g^+t^2)$	5.72	$(t^4g^+t)t(t^4g^+t)$	5.41	$(t^4g^+t)t(t^3g^+t^2)$ (tg^+t)	4.35
$(t^5g^+)t(t^3g^+t^2)$	2.57	$(t^5g^+)t(t^4g^+t)$	1.98	$(t^5g^+)t(t^3g^+t^2)$ (tg^+t)	.98
$(t^6)t(t^3g^{+2}t)$	4.32	$(t^6)t(t^6)$	5.05	$(t^6)t(t^3g^{+2}t)$ (t^3)	3.81
$(g^+t^5)t(t^3g^{+2}t)$	3.85	$(g^+t^5)t(t^6)$	4.67	$(g^+t^5)t(t^3g^{+2}t)$ (t^3)	3.23
$(tg^+t^4)t(t^3g^{+2}t)$	3.05	$(tg^+t^4)t(t^6)$	4.09	$(tg^+t^4)t(t^3g^{+2}t)$ (t^3)	2.33
$(t^2g^+t^3)t(t^3g^{+2}t)$	3.76	$(t^2g^+t^3)t(t^6)$	4.67	$(t^2g^+t^3)t(t^3g^{+2}t)$ (t^3)	3.18
$(t^3g^+t^2)t(t^3g^{+2}t)$	2.19	$(t^3g^+t^2)t(t^6)$	3.48	$(t^3g^+t^2)t(t^3g^{+2}t)$ (t^3)	1.44
$(t^4g^+t)t(t^3g^{+2}t)$	5.32	$(t^4g^+t)t(t^6)$	6.54	$(t^4g^+t)t(t^3g^{+2}t)$ (t^3)	4.73
$(t^5g^+)t(t^3g^{+2}t)$	1.50	$(t^5g^+)t(t^6)$	3.88	$(t^5g^+)t(t^3g^{+2}t)$ (t^3)	1.11
$(t^6)t(tg^+tg^{+2}t)$	5.37	$(t^6)t(tg^+t^4)$	6.54	$(t^6)t(tg^+tg^{+2}t)$ (t^3)	4.83
$(t^6)t(g^+t^2g^{+2}t)$	3.55	$(t^6)t(g^+t^5)$	3.88	$(t^6)t(g^+ttg^{+2}t)$ (t^3)	3.43

Table IX. Test of an empirical relationship between k_b, k_A and k_B. $\alpha = k_Ak_B[k_b(k_A + k_B)]^{-1}$

Tables	Configurations	Average α	Standard Deviation
IV	28	0.84	0.13
V	33	0.85	0.19
VI	21	1.04	0.89
VII	23	0.70	0.12
VIII	23	0.90	0.30
IV, V, VII, VIII	107	0.80	0.20
IV, V, VI, VII, VIII	128	0.84	0.41
VI*	20	0.90	0.36
VI*	19	0.79	0.19
IV, V, VI*, VII, VIII	126	0.80	0.20

*Averages obtained after deletion of one or two of the configurations listed in Table VI.

should emerge unscathed if a more realistic potential model were used.

A discussion of the influence of branching on barrier heights is deferred to the end of this section.

All initial state configurations listed in Tables IV–VIII are of the form given in 1. For the most part, we have only listed conformations with g^+ states. Configurations where g^- replaces g^+ show identical qualitative trends and provide no new insight. A careful study of these tables allows us to draw these conclusions.

(C-1) Overall the net effect is to make the branched tail **1a** behave akin to a rigid conformation and thereby, the P configuration exerts the major influence on the transition rate. The range of transition rates spanned by branched molecules is quite close to that spanned by the linear molecule, P-t-Q_0Q_1, counterpart.

(C-2) For a given P-t-Q_0Q_1 conformation, the further the attached branch is from the transforming bond, the faster is the transition rate.

(C-3) If P-t-Q_0Q_1 and B remain fixed, the smaller the number of vertices in the attached branch Q_2, the faster the transition rate becomes.

Once a particular P configuration is chosen, the qualitative effect of gauche bond placement and variation is identical with that in linear molecules.

Many of the entries in Tables IV–VIII suggest the transition rate in the branched molecule might be approximated by a relationship reminiscent of $k_b^{-1} = k_A^{-1} + k_B^{-1}$, where k_A and k_B are the rates in the two isolated unbranched chains and k_b is the transition rate in the branched molecule. In order to assess the usefulness of this type of approximation, define α for a given configuration as

$$\alpha = k_Ak_B[k_b(k_A + k_B)]^{-1} \tag{IV.7}$$

Is α approximately the same for all configurations, and, if so, what is its average value? Table IX lists the average of α, and the standard deviation, for configurations listed in each of the Tables IV–VIII.

Table VI stands out immediately as markedly different from the other four. While the average α is 0.70–0.85 for Tables IV, V, VII, and VIII, it rises to 1.04 for Table VI. An even more dramatic difference is seen in the standard deviation, which is 0.12–0.30 for Tables IV, V, VII, and VIII, but 0.89 for Table VI. Another means of showing the unique character of Table VI is to compare average α, and standard deviations, for all five tables and for all tables except Table VI. This information is listed as the sixth and seventh entries in Table IX. The standard deviation doubles (from 0.20 to 0.41) when Table VI is included in the averaging.

The peculiar character of Table VI is a consequence of only two of its 21 configurations, as is shown by the eighth and ninth entries in Table IX. If two of the entries in Table VI are ignored, the average α for this table is 0.79 and the standard deviation is only 0.19. Hence the empirical relationships

$$k_b = k_A k_B [0.8(k_A + k_B)]^{-1} \qquad \text{(IV.8)}$$

will produce *most* k_b to an accuracy which merits a standard deviation of about 25%. There will be a few configurations, however, for which eq IV.8 is grossly in error.

The two configurations in Table VI which are poorly represented by eq IV.8 are those listed as the fifth and seventh entries. In both cases the actual k_b is much smaller than the estimate provided by eq IV.8. P is rigid for both of these configurations, but Q_0Q_1 and Q_0Q_2 individually are flexible. Therefore reasonably high transition rates are obtained for chain A and chain B. The combined branched tail, with a branch near the transforming bond, however, becomes rigid. In combination with the rigid P, the rigid branched tail produces a low rate for the transition in the branched molecule.

We now examine the possible influence of a more realistic chain potential on the preceding conclusions established for transitions of the variety 1. A torsional potential that explicitly links vertices at and near the branch point will act to make the tail even more rigid. Thus, observation C-1 is enhanced and we would anticipate no change in our qualitative observations.

The effect on k_b of a more sophisticated torsional potential that takes account of the nearest-neighbor rotational states influence on the barrier height of the transforming bond is considered below. At the lowest level of approximation, assume that the torsional potential in a branched molecule is the sum of the independent torsional potentials of each branch and that the barrier height depends on the nearest-neighbor conformation. Such a potential function will again give the qualitative results B-1 and C-1. While the calculated transition rates for branched as well as linear alkanes will be different from these obtained here, the ratio of the transition rates will be the same. Of far greater importance is the effect of an attached branch on the barrier height of the transforming bond. At the level of approximation employed here, we need only concern ourselves with initial states of type 2, i.e., where the attached branch is at the transforming bond. To obtain a rough estimate of the influence of an attached branch on barrier height, let us consider some experimental data on short alkanes. In $CH_3CH_2CH_3$ the rotational barrier as determined from IR spectroscopy[32] is reported to be 3.4 kcal/mol. The disubstituted alkane $CH_3CH_2(CH_3)_2$ is reported to have an internal rotational barrier of 3.6[33] to 3.9[34] kcal/mol. Taking the increased barrier height to be 0.5 kcal/mol and assuming the torsional curvature remains unchanged result in a 50% reduction in k_b at 372 K. (Using eq III.1, the reader can obtain an approximate transition rate by inserting the barrier height deemed appropriate.) Thus, we expect the qualitative conclusion that the time scale of conformational transitions is about the same in branched and linear alkanes should remain unchanged when a more realistic treatment of branching effects on the torsional potential is employed.

In a branched molecule, the angle bending force constants associated with the two bond angles θ_B and θ_{M-1} at vertex B are not the same as at an unbranched vertex; rather they would be expected to be larger.[28,35] However, the dominant distortion in the localized mode occurs in the torsional degrees of freedom and to a lesser degree in the angle bending modes, and a somewhat increased value of γ_θ should not exert a drastic influence on k_b. For example, in the rigid conformation $(t^5g^+)t(g^+t^5)$, where angle bending is important, a tenfold increase in all the bond angle bending force constants only changes the transition rate from 0.60 to 0.36 ns^{-1}. Moreover, it seems intuitively reasonable than an increased value of $\gamma_{\theta,B}$ and $\gamma_{\theta,M-1}$ will act to further increase the branched tail rigidity. Consequently, the introduction of a more realistic angle bending potential is not expected to significantly alter the qualitative conclusions of this work.

V. Conclusions

In the context of the multidimensional Kramers rate theory, we have investigated the effect of chain branching on the mechanism and rates of conformational transitions. Not surprisingly, we find that the presence of a side chain introduces rigidity into one of the tails attached to the transforming bond and can be viewed in an analogous fashion to a "rigid" conformation in the linear molecule. Overall, while the presence of additional vertices in a branched molecule somewhat diminishes the transition rate, the effect is minor; conformational transitions occur on the same time scale in branched molecules as in their linear counterparts. Thus, one need merely study the far simpler linear chain molecules to gain insight into mechanism and rates of conformational transitions in branched chains.

Our studies on branched molecules imply that the treatment of methylene groups as a single sphere (vertex) is a good approximation in the calculation of transition rates. Surely, if the bulkier attached methylene vertices exert a relatively minor influence on transition rates, the presence of an attached hydrogen or two should give a minimal effect. In a similar fashion, the presence of side chains containing several methylene spheres is expected to produce a fairly small decrease in the transition rate of a main-chain bond.

It would prove useful if Brownian dynamics simulations were done on branched molecules to test the predictions presented here. On the basis of our experience with linear chains, we expect the qualitative results to articulate with the simulation; although due to cooperativity, simulated transition rates will probably be somewhat faster.

Acknowledgment. This work was supported in part by National Science Foundation Grant PCM 78-22916. Acknowledgment is also made to the donors of the Petroleum Research Fund, administered by the American Chemical Society, for partial support of this research.

Miniprint Material Available: Full-size photocopies of Tables I–IX (18 pages). Ordering information is given on any current masthead page.

References and Notes

(1) Bauer, D. R.; Brauman, J. I.; Pecora, R. *Macromolecules* **1975**, *8*, 443.
(2) Basal, B.; Lowry, A.; Yu, H.; Stockmayer, W. H. In "Dielectric Properties of Polymers"; Karasz, F. E., Ed.; Plenum Press: New York, 1972.
(3) Morawetz, H. *Acc. Chem. Res.* **1970**, *3*, 354.
(4) Lauprêtre, F.; Noël, C.; Monnerie, L. *J. Polym. Sci., Polym. Phys. Ed.* **1977**, *15*, 2143.
(5) Valeur, B.; Monnerie, L. *J. Polym. Sci., Polym. Phys. Ed.* **1976**, *14*, 29.
(6) Helfand, E.; Wasserman, Z. R.; Weber, T. A. *J. Chem. Phys.* **1979**, *70*, 2016.
(7) Helfand, E.; Wasserman, Z. R.; Weber, T. A. *Macromolecules* **1980**, *13*, 526.
(8) Weiner, J. H.; Pear, H. R. *Macromolecules* **1977**, *10*, 317.
(9) Fixman, M. *J. Chem. Phys.* **1979**, *69*, 1527, 1538.
(10) Robertas, D. W.; Berne, B. J.; Chandler, D. *J. Chem. Phys.* **1979**, *70*, 3397.
(11) Fixman, M.; Evans, G. T. *J. Chem. Phys.* **1978**, *68*, 195.
(12) Adler, R. S.; Freed, K. F. *J. Chem. Phys.* **1980**, *72*, 2032.
(13) Skolnick, J.; Helfand, E. *J. Chem. Phys.* **1980**, *72*, 5489.
(14) Axelson, D. E.; Levy, G. L.; Mandelkern, L. *Macromolecules* **1979**, *12*, 41.
(15) Dorman, D. E.; Otocka, E. P.; Bovey, F. A. *Macromolecules* **1972**, *5*, 574.
(16) Cudby, M. E. A.; Bunn, A. *Polymer* **1976**, *17*, 345.
(17) Bovey, F. A.; Schilling, F. C.; McCrackin, F. L.; Wagner, H. L. *Macromolecules* **1976**, *9*, 76.
(18) Cheng, H. N.; Schilling, F. C.; Bovey, F. A. *Macromolecules* **1976**, *9*, 363.
(19) Bowmer, T. N.; O'Donnell, J. H. *Polymer* **1977**, *18*, 1032.
(20) Zimm, B. H.; Stockmayer, W. H. *J. Chem. Phys.* **1949**, *17*, 1301.
(21) Orofino, T. A. *Polymer* **1961**, *2*, 305.
(22) Tonelli, A. E. *J. Am. Chem. Soc.* **1972**, *94*, 2972.
(23) Mattice, W. L.; Carpenter, D. K. *Macromolecules* **1976**, *9*, 53.
(24) Mattice, W. L. *Macromolecules* **1978**, *11*, 517.
(25) Solc, K. *Macromolecules* **1973**, *6*, 378.
(26) Mattice, W. L. *Macromolecules* **1977**, *10*, 1182.
(27) Mattice, W. L. *Macromolecules* **1980**, *13*, 506.
(28) Flory, P. J. "Statistical Mechanics of Chain Molecules"; Interscience: New York, 1969.
(29) Blomberg, C. *Chem. Phys.* **1979**, *37*, 219. See also: Brinkman, H. C. *Physica* **1956**, *22*, 149. Landauer, R.; Swanson, J. A. *Phys. Rev.* **1961**, *121*, 1668. Langer, J. S. *Ann. Phys.* **1969**, *54*, 258.
(30) Kramers, H. A. *Physica* **1940**, *7*, 284.
(31) For a comparison with linear alkanes, see Tables II, VII, and VIII of ref 13.
(32) Pitzer, K. S. *Discuss. Faraday Soc.* **1951**, *10*, 66.
(33) Linde, D. R. *J. Chem. Phys.* **1958**, *29*, 1426.
(34) Linde, D. R.; Mann, D. E. *J. Chem. Phys.* **1958**, *29*, 914.
(35) Pitzer, K. S. *J. Chem. Phys.* **1940**, *8*, 711.

Studies on Orientation Behavior of Poly(γ-benzyl L-glutamate) in an Electric Field by means of Small-Angle Light Scattering[1a]

Fumihiko Ozaki,[1b] Tetsuya Ogita,[1b] and Masaru Matsuo*[1c]

Department of Textile Engineering, Faculty of Home Economics, Nara Women's University, Nara 630, Japan, and Department of Textile Engineering, Faculty of Engineering, Yamagata University, Yonezawa 992, Japan.

Received July 23, 1980

ABSTRACT: The orientation behavior of liquid crystalline solutions of poly(γ-benzyl L-glutamate) in chloroform in an electric field was studied by means of small-angle light scattering, the polarizing microscope, and birefringence measurements. The experimental results indicate that the molecular aggregate has a rodlike texture and that the optical axes within the rod are oriented in the electric field direction. In order to study the variation of the light scattering patterns with increasing electric field, we have carried out theoretical calculations by introducing parameters associated with the magnitudes of the optical anisotropy disorder and of the orientation disorder of the optical axes of the scattering elements. Models were proposed in two cases in which the incident beam was parallel and perpendicular to the direction of the electric field. With a proper choice of parameters, the calculated results were found to be rather close to those observed. On this basis, it was concluded that the degree of ordering of the optical axes within the rod increases with increasing electric field.

Introduction

It is well-known that liquid crystals of poly(γ-benzyl L-glutamate) (PBLG) are oriented in electric[2-11] and magnetic fields.[12-16] The orientation behavior has been mainly investigated by means of the polarizing microscope,[2] transient electric birefringence,[10-12] small-angle light scattering,[6,16] and X-ray diffraction techniques.[3,15] Since Robinson[17-19] reported the liquid crystal nature of synthetic polypeptides, these techniques have made clear the orientation behavior of PBLG. Toth and Tobolsky[2] studied the electric orientation of liquid crystalline solutions (15% w/v) of PBLG of molecular weight 310 000 by the polarizing microscope method. They reported that the light transmitted through the sample decreases with increasing electric field when the direction of the incident beam is parallel to the electric field.

Iizuka et al. have studied the orientation behavior of liquid crystalline solutions in electric fields, using small-angle light scattering[6] and infrared dichroic ratios,[4,5] in which the incident beam was perpendicular to the electric field. Wilkes[16] has interpreted the morphology of PBLG films cast from chloroform solutions (that were no older than 1 month) on the basis of the light scattering model proposed by Rhodes and Stein.[20] Using thin films in a 16.5-kG magnetic field, he reported that the molecular clusters, assuming them to have the so-called rodlike texture, were oriented perpendicular to the magnetic field rather than parallel. The theoretical treatment of light scattering from polymer films was developed by Stein, who with his co-workers has reported a number of studies of the small-angle light scattering from unoriented and oriented films[21-24] and from liquid crystals of PBLG.[25,26] They provided a quantitative interpretation[25] of the effect of optical rotation on small-angle light scattering in a system in which polystyrene spherulites were surrounded by an optically active medium consisting of a concentrated

0024-9297/81/2214-0299$01.25/0